Phase Patterning in Multi-stable Metamaterials: Transition Wave Stabilization and Conversion

Chongan Wang and Michael J. Frazier[a)]
Department of Mechanical and Aerospace Engineering, University of California, San Diego, California 92093, USA

(Dated: 31 March 2023)

This letter proposes a novel metamaterial design strategy leveraging a tunable structural defect for manipulating the propagation of transition waves toward custom multi-phase patterning in multi-stable mechanical metamaterials. The defect reversibly adjusts the on-site potential in order to affect the motion of the transition waves which traverse it, either prohibiting wave transmission (i.e., stabilization) or permitting transmission of specific modes, possible converting one mode into another. Thus, the defect is able to control the occurrence and distribution of the structural phases and realize the desired phase patterns. Although the metamaterial model for our analytical and numerical study is a one-dimensional (1D) architecture comprising tri-stable elements, the proposed method is shown to apply to 2D architectures and is amenable to elements possessing more than three stable states, demonstrating greater flexibility in metamaterial design than current approaches. The proposed method expands the configuration space of phase-transforming metamaterials, which contributes to efforts aimed at re-programmable mechanical/dynamic performance.

Phase transformations are a prominent mechanism of equilibration in materials whose microstructure exhibits more than one energetically stable configuration (i.e., phase)[1]. Within a given material sample, regions of differing configuration (i.e., domains) may coexist, delimited by an interpolating interface (i.e., domain wall) whose motion constitutes a transition wave effectuating the transformation from one phase to another. The physical properties can vary drastically between domains of differing phase and even within the domain walls, affecting the macroscopic material behavior. Managing the occurrence and distribution of the disparate phases within a material sample (i.e., phase patterning) via deft domain wall control is at the core of many current and emerging information technologies[2–5] and, thus, attracts significant research attention.

Intriguingly, analogous transformation phenomena have been elicited at the structural level from engineered media – mechanical metamaterials – comprising multi-stable elements and, likewise, have realized novel functionalities and diverse applications[6–10] The accessibility of the internal architecture permits a variety of metamaterial designs[11–15] for a tailored response; yet, with rare exception[16–19], most designs are one-dimensional (1D) systems of identical bi-stable elements within which transition waves transform the entire structure from the (high-energy) meta-stable phase to the (low energy) ground state, demonstrating a severely limited global configuration space compared to that currently exploited in traditional phase-transforming materials.

Recently, utilizing bi-stable elements with energetically-degenerate, though mechanically distinct ground states, Ramakrishnan and Frazier[20] realized stable, defect-mediated phase patterns within a 1D structure. Since the constituent phases were mechanically distinct, the system dynamic response was shown to be affected by the tuned patterning, enabling the realization of waveguides with variable pass band. Alternatively, utilizing tri-stable elements with two degenerate ground states, Yasuda *et al.*[21] demonstrated stable patterns of the ground-state configurations upon the collision of incompatible wavefronts. Likewise, the global mechanical properties were shown to be affected by the specific phase patterning; in particular, the number and distribution of domain walls since the intervening domains were mechanically identical. While these efforts are noteworthy for introducing the patterning concept to the metamaterial platform, we identify two constraints inherent to each approach that inhibit opportunities to achieve more complex morphologies: for pattern stability, there is the apparent requirement for (i) the on-site potential to possess energetically-degenerate states and (ii) the metamaterial architecture to be 1D. Thus far, patterns have also been restricted to two phases, the minimum number.

In this letter, we present a design strategy to achieve stable structural phase patterns in multi-stable metamaterials with tunable defects. In implementing the defects, our objective is to reversibly alter the on-site potential driving transition waves in order to control the occurrence, distribution, and stability of phases, which involves the immobilization of domain walls and the conversion of propagating waves from one mode to another. The conversion of one propagating mode into another is new to the metamaterial literature related to transition waves but appears in other contexts[22,23]. The proposed strategy neither relies on energetically-degenerate states nor is limited to 1D architectures and can accommodate multi-stable potentials for patterning more than two phases.

Our point of departure is the one-dimensional (1D)

[a)]Corresponding author email: mjfrazier@ucsd.edu

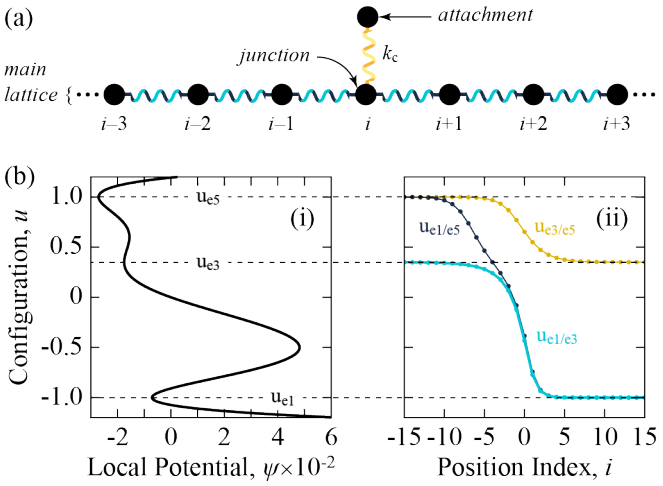

FIG. 1. (a) One-dimensional (1D) chain of tri-stable elements with anomalous attachment. (b) (i) Tri-stable on-site potential. (ii) Waveforms of three possible transitions: $u_{e1/e3}$, $u_{e3/e5}$, and $u_{e1/e5}$. The proposed method affects only the $u_{e1/e3}$ and $u_{e1/e5}$ modes.

metamaterial comprising tri-stable elements depicted in Fig. 1a. Within this architecture, we distinguish the main lattice that comprises identical, elastically-coupled elements with single displacement degree of freedom, u_i, $i \in \mathbb{Z}$, and the local attachment, an anomalous element with displacement freedom, u_L, coupled to a single site (i.e., the *junction*) within the lattice interior. For simplicity, the tri-stability of each element is described by the same form of potential function, $\psi(u)$; however, crucially, that of the local attachment is amplified by a factor, K. The relevant non-dimensional discrete governing equations with on-site viscous damping, η, are given by [SI]:

$$\ddot{u}_i + \eta\dot{u}_i + (2u_i - u_{i+1} - u_{i-1}) + \psi'(u_i)\cdots + \sum_I k_c(u_0 - u_L)\delta_{Ii} = 0, \quad \text{(1a)}$$

$$\ddot{u}_L + \eta\dot{u}_L + K\psi'(u_L) + k_c(u_L - u_I) = 0, \quad \text{(1b)}$$

where k_c denotes the coupling stiffness between the local attachment and the main lattice. The function, δ_{Ii}, is the Kronecker delta and, in the case of multiple attachments, I collects the indices of elements within the main lattice to which the attachments are singularly coupled. In the following, $I = 0$ and u_0 designates the displacement of junction element.

The tri-stable potential function emerges from the integration of

$$\psi'(u) = \prod_{i=1}^{5}(u - u_{ei}), \quad (2)$$

where u_{ei} are the equilibrium configurations; likewise, $\psi_{ei} = \psi(u_{ei})$ are the corresponding free energies of the equilibria. In order to support different transition wave modes, we desire $\psi(u)$ be asymmetric. Here, we consider the case where $(u_{e1}, u_{e2}, u_{e3}, u_{e4}, u_{e5}) = (-1, -1/2, 7/20, 3/5, 1)$ which generates a tri-stable potential with stable states of progressively lower energy (i.e., $\psi_{e1} > \psi_{e3} > \psi_{e5}$) as well as monotonically decreasing energy barriers (i.e., $\psi_{e2} > \psi_{e4}$) (Fig. 1b.i). This condition ensures that all back- and forward-propagating transition waves exhibit kink and anti-kink profiles, respectively. The condition is one of convenience rather than functional necessity since it permits the theoretical discussion to proceed with reference to only one waveform with the understanding that it is a mere reflection of the other. Here, we utilize tri-stable elements; however, the approach outlined below readily extends to the case of n-stable ($n \geq 3$) elements, permitting patterns comprising as many as n phases. For the lattice initially uniform in $u_i = u_{e1}$, phase transformation is effectuated by one of two transition wave modes: $u_{e1/e3}$ and $u_{e1/e5}$ where $u_{ei/ej}$ represents the transition form the u_{ei} to the u_{ej} phase (Fig. 1b.ii).

Following a set of criteria, below, we design the local attachment to modify the on-site potential of the junction according to the present configuration, u_L, such that the incoming transition wave is either immobilized at the junction, transmitted unaltered, or transmitted as another wave mode (i.e., converted). In short, regardless of the incoming transition wave, in the domain beyond the junction, we desire that the equilibrium phase match the prescribed configuration of u_L. To this end, we theoretically determine the attachment parameters realize the desired performance. For numerical verification, we simulate the transition wave motion in the system described by Eq. (1) with $\eta = 3/5$. The system size, $N = 101$, is more than sufficient to ensure that, following initiation at the left boundary, the transition wave (anti-kink) profile and velocity reach a steady-state before the influence of the junction becomes apparent. The lattice-attachment coupling stiffness, k_c, is to be determined.

To simplify the theoretical analysis, we assume that $K \to \infty$ such that u_L is a parameter to be prescribed (i.e., $u_L = \{u_{e1}, u_{e3}, u_{e5}\}$) rather than a variable to be determined. Nevertheless, the simulations set $K = 40$. With a sufficiently large K, u_L affects u_0 via k_c but the reciprocal is, effectively, avoided. In this case, the local attachment acts as a tunable boundary condition of the main lattice. A discussion on the analytical implications of a finite K is presented in the SI. For the lattice initially uniform in $u_i = u_{e1}$, we desire that the attachment configuration regulate the transition wave mode that is transmitted across the junction. The behavior is summarized by the following criteria:

(i) The prescription of $u_L = \{u_{e3}, u_{e5}\}$ does not stimulate a transition wave.

(ii) For $u_L = u_{e5}$, the incoming $u_{e1/e5}$ transition wave is transmitted across the junction while the $u_{e1/e3}$ wave is converted to the $u_{e1/e5}$ mode.

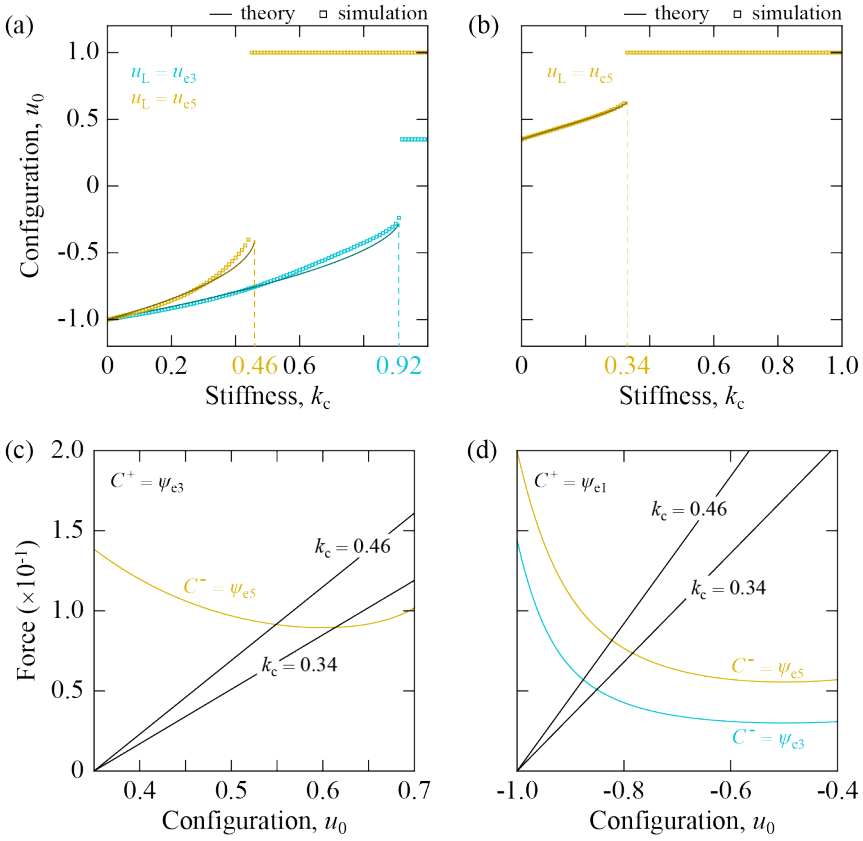

FIG. 2. Attachment Calibration. Attachment stiffness and junction response for a static field with (a) $C^+ = C^- = \psi_{e1}$ and $u_L = \{u_{e3}, u_{e5}\}$ [criterion (i)] and (b) $C^+ = C^- = \psi_{e3}$ and $u_L = u_{e5}$ [criterion (ii)]. Each side of Eq. (9) plotted separately assuming (c) $C^+ = \psi_{e3}$ and $C^- = \psi_{e5}$ [criterion (iii)] and (d) $C^+ = \psi_{e1}$ and either $C^- = \psi_{e3}$ or $C^- = \psi_{e5}$ [criterion (iv)].

(iii) For $u_L = u_{e3}$, the incoming $u_{e1/e3}$ transition wave is transmitted across the junction while the $u_{e1/e5}$ wave is converted to the $u_{e1/e3}$ mode.

(iv) For $u_L = u_{e1}$, all incoming transition waves are immobilized at the junction.

Since u_L is prescribed, k_c is the only parameter yet to be determined in accordance with the above criteria. For an analytical determination, we are aided by the continuum form of Eq. (1) derived by expanding $u_{i\pm1}$ in Taylor series to second order:

$$u_{,tt} + \eta u_{,t} - u_{,xx} + \psi'(u) + k_c(u_0 - u_L)\delta(x) = 0, \quad (3)$$

where $u_0 = u(0)$ is the configuration of the junction and $\delta(x)$ is the Dirac delta function. Each criterion implies a unique steady-state configuration of the lattice; consequently, we study the time-independent form of Eq. (3):

$$-u_{,xx} + \psi'(u) + k_c(u_0 - u_L)\delta(x) = 0. \quad (4)$$

Since $\delta(x)$ is not bounded, u is continuous but not differentiable at the junction. The gradient on either side of the discontinuity is computed by integrating Eq. (4) in the range $x \in [0^-, 0^+]$, yielding

$$u_{,x}(0^-) - u_{,x}(0^+) + k_c(u_0 - u_L) = 0. \quad (5)$$

On the other hand, multiplying Eq. (4) by $u_{,x}$ and integrating yields the first integral of motion:

$$-\frac{1}{2}u_{,x}^2 + \psi(u) = \begin{cases} C^+ & x > 0, \\ C^- & x < 0, \end{cases} \quad (6)$$

which is piecewise constant due to the discontinuity in $u_{,x}$ at $x = 0$. Nevertheless, given that $\lim_{x\to\pm\infty} u_{,x} = 0$, the $C^\pm$ are identical to the equilibrium potential in the remotes region, i.e., $C^\pm = \psi[u(x = \pm\infty)]$. Consequently, from Eq. (6):

$$-\frac{1}{2}[u_{,x}(0^+)]^2 + \psi(u_0) = C^+ = \psi_{ei}, \quad (7a)$$

$$-\frac{1}{2}[u_{,x}(0^-)]^2 + \psi(u_0) = C^- = \psi_{ej}, \quad (7b)$$

where $i, j = \{1, 3, 5\}$. Together, Eqs. (5) and (7) form a complete set of algebraic equations for the system in steady state. From these equations, we are able to derive two relations for the conditions $C^+ = C^-$ and $C^+ \neq C^-$, respectively [SI]. The former represents the scenario in

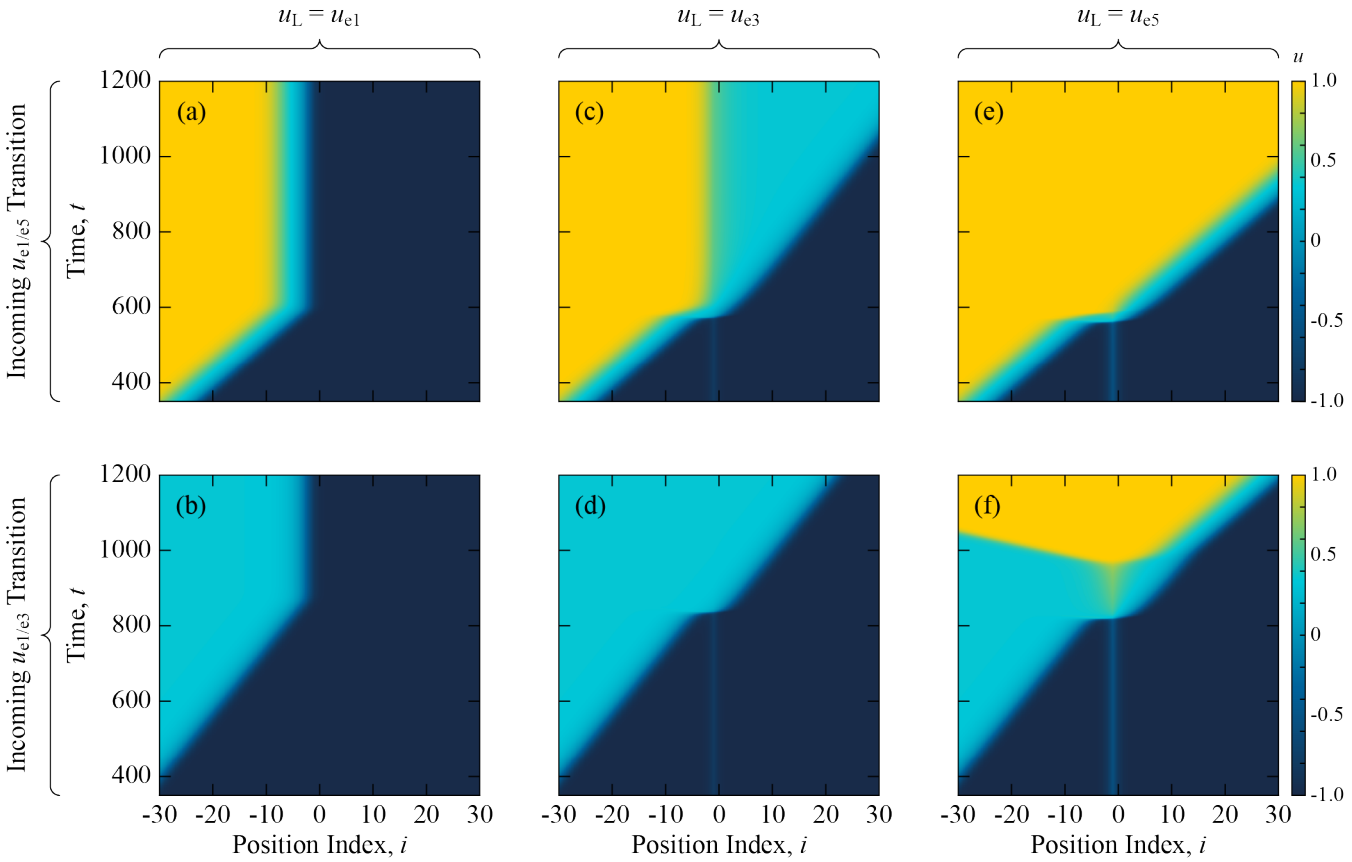

FIG. 3. Transition Wave Stabilization and Conversion. Spatio-temporal evolution of $u_{e1/e5}$- and $u_{e1/e3}$-mode transition waves in the lattice with prescribed $u_L = \{u_{e1}, u_{e3}, u_{e5}\}$, demonstrating wave stabilization and conversion according to the stated criteria in the text.

which the lattice perturbed from the uniform state by the local attachment and yields:

$$\psi(u_0) = \psi_{ei} + \frac{k_c^2}{8}(u_0 - u_L)^2. \quad (8)$$

The latter corresponds to the case in which, as an effect of the local attachment, a transition wave is immobilized at the junction and yields (assuming an anti-kink wave profile):

$$-\sqrt{2[\psi(u_0) - \psi_{ei}]} + \sqrt{2[\psi(u_0) - \psi_{ej}]} = k_c(u_0 - u_L), \quad (9)$$

where $\psi_{ei} > \psi_{ej}$ and $u_L = u_{ei}$. Equation (8) expresses an energy balance while Eq. (9) a force balance. These are the main theoretical results.

In light of Eqs. (8) and (9) and the above criteria, we determine the a suitable value for k_c. We compare the theoretical predictions based upon the continuum model [Eqs. (8) and (9)] to the numerical results from simulations of the discrete model [Eq. (1)] for $u_L = \{u_{e1}, u_{e3}, u_{e5}\}$ and a parametrically increasing k_c.

First, we consider criterion (i) for which $u_L = \{u_{e3}, u_{e5}\}$ does not trigger a transition wave in the lattice initially uniform in $u_i = u = u_{e1}$ (thus, $C^{\pm} = \psi_{e1}$). Figure 2a plots the (k_c, u_0) solution of Eq. (8), indicating that, for $u_L = u_{e3}$, the equality is maintained by $k_c \in [0, 0.92)$; for $u_L = u_{e5}$, the equality is maintained by $k_c \in [0, 46)$. The theoretical findings are supported by the numerical results which exhibit a discontinuity in the steady-state u_0 at $k_c \approx 0.91$ under $u_L = u_{e3}$ and $k_c \approx 0.44$ under $u_L = u_{e5}$, signaling sufficient coupling to initiate a transition wave within the main lattice. The analytical-numerical agreement validates the theoretical approach. Since criterion (i) mandates that no transition wave shall be initiated by $u_L = \{u_{e3}, u_{e5}\}$, $k_c \approx 0.46$ is the maximum allowable stiffness.

Next, we consider criterion (ii) for which setting $u_L = u_{e5}$ has no lasting affect on the $u_{e1/e5}$ wave profile as it traverses the junction, while converting the incoming $u_{e1/e3}$ wave to the $u_{e1/e5}$ mode. Criterion (ii) implies that the lattice uniform in $u_i = u = u_{e3}$ (thus, $C^{\pm} = \psi_{e3}$) (as if following the passage of a $u_{e1/e3}$ wave) is unstable under $u_L = u_{e5}$. Figure 2b plots the (k_c, u_0) solution of Eq. (8) for $k_c \in [0, 0.34)$. Since the equality fails for $k_c > 0.34$, the lattice uniform in u_{e3} and under $u_L = u_{e5}$ is unstable such that the incoming $u_{e1/e3}$ transition wave is converted to the $u_{e1/e5}$ mode upon traversing the junction. Excellent agreement is observed

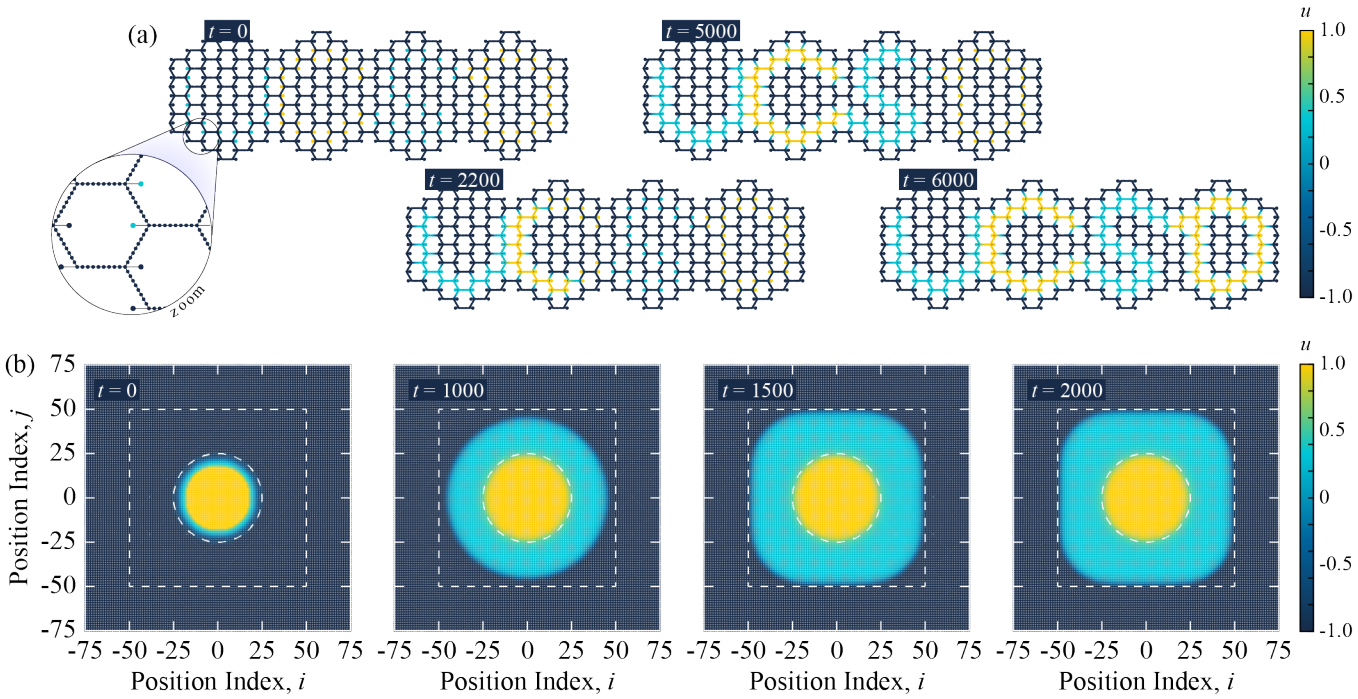

FIG. 4. Phase Patterning in 2D Architectures. (a) A hierarchical hexagonal lattice of tri-stable elements with tunable attachment at the corner junctions. From the uniform u_{e1} state, a transition wave stimulated at $\star$ is guided and converted by the attachments to produce the desired phase morphology. (b) A square lattice where attachments on elements along the perimeter of inscribed shapes (delineated by dashed lines) create the desired phase morphology. Without the attachments, merely prescribing the phases patterns in (a,b) would not produce stable multi-phase morphologies.

between the theoretical and numerical results, where a discontinuity in u_0 occurs at $k_c \approx 0.32$. Thus, $k_c \approx 0.34$ is the minimum stiffness that satisfies criterion (ii).

Together, criteria (i) and (ii) narrow the range of stiffness, $k_c \in (0.34, 0.46)$; a result determined by considering the stability of the uniform lattice perturbed by u_L. This uniformity was manifest in Eq. (7) as $C^+ = C^-$ and, ultimately, a single value of ψ_{ei} in Eq. (8). For criterion (iii), converting the $u_{e1/e5}$ wave to the $u_{e1/e3}$ mode at the junction implies the steady-state condition in which a domain wall is pinned at the junction, interpolating phases u_{e5} ($x < 0$) and u_{e3} ($x > 0$); thus, $C^+ \neq C^-$ and $\psi_{ei} \neq \psi_{ej}$ in Eq. (9). A similar situation arises in satisfying criterion (iv) since the domain wall of every transition wave is pinned to the junction. Each side of Eq. (9) is plotted in Fig. 2c,d for criteria (iii) and (iv), respectively. Apparently, any $k_c \in (0.34, 0.46)$ that satisfies criteria (i) and (ii) also maintains the equality in Eq. (9) and, thus, satisfies criteria (iii) and (iv), as well.

To validate the analysis, we provide numerical examples of transition wave stabilization and conversion in Fig. 3, which depicts the spatio-temporal evolution of $u_{e1/e5}$ and $u_{e1/e3}$ transition waves stimulated from the left boundary of a lattice with coupled attachment in configuration $u_L = \{u_{e1}, u_{e3}, u_{e5}\}$. We select $k_c = 0.4$ from within the criteria-mediated stiffness range. Apparently, all the criteria are met: setting $u_L = \{u_{e3}, u_{e5}\}$ does not initiate a transition wave from the junction (Figs. 3c–f) [criterion (i)]; setting $u_L = u_{e5}$ does not generate any lasting effects for passing $u_{e1/e5}$ waves, but converts incoming waves of $u_{e1/e3}$ to $u_{e1/e5}$ (Fig. 3e,f) [criterion (ii)]; setting $u_L = u_{e3}$ does not generate any lasting effects for passing $u_{e1/e3}$ waves, but converts incoming waves of $u_{e1/e5}$ to $u_{e1/e3}$ (Fig. 3c,d) [criterion (iii)]; setting $u_L = u_{e1}$ immobilizes all transition waves at the junction (Figs. 3a,b) [criterion (iv)]. In Fig. 3f, we note that in converting a wave of $u_{e1/e3}$ to $u_{e1/e5}$, a back propagating wave of the $u_{e3/e5}$ mode is also stimulated. If, in practice, this is undesirable, then a second attachment coupled to a lattice site $i < 0$ and maintained in state, $u_L = u_{e3}$, may prevent the back propagation (see Fig. S7 in the SI). Nevertheless, the tunable attachment is shown to regulate the distribution of multiple phases, demonstrating a patterning ability.

Although the above investigation focuses on 1D metamaterial structures, the method of tunable defects extends phase patterning, for the first time, to 2D structures, as well. To demonstrate this numerically, we consider transition wave propagation within the 2D hierarchical hexagonal lattice depicted in Fig. 4a where each lattice segment comprises a 1D chain of ten tri-stable elements and each corner element (i.e., junction) is adorned with a local attachment coupled through $k_c = 0.6$ [SI]. The independently-tunable attachments ensure that the transition wave approaching

the junction is either immobilized there, transmitted unaltered, or converted to another mode in order to realize an improvised multi-phase pattern. We also present the non-hierarchical square lattice with nearest-neighbor interactions depicted in Fig. 4b within which a subset of lattice sites couple to a tunable attachments ($k_c = 0.4$): along the perimeter of a circle of radius, $R = 25$, attachments are set to $u_L = u_{e3}$; along the perimeter of a square of side length, $L = 100$, attachments are set to $u_L = u_{e1}$. Within a u_{e1} background, an initial circular phase of u_{e5} expands to the circular boundary where the $u_{e1/e5}$ wavefront is converted to the $u_{e1/e3}$ mode following the attachment prescription. Subsequently, the $u_{e1/e3}$ wave expands until stabilized by attachments at the square boundary.

In summary, we have developed a method utilizing tunable soft defects for patterning stable structural phases in mechanical metamaterials comprising multi-stable elements. Compared to previous strategies, the proposed approach grants additional design flexibility in forgoing a reliance on degenerate ground states and in extending the patterning capability to 2D architectures suited to complex morphologies. As each phase may be associated with unique on-site stiffness, the defect-enabled patterning may realized meso-scale morphologies to deliberately affect the macroscopic metamaterial mechanics/dynamics. Similarly, as each phase constitutes a unique structural configuration, the method may assist in the realization of deformation patterns for morphing surfaces. While the inherent multi-stability of soft defects upholds the tuned state, in practice, the switching between tuned states may be shrewdly accomplished via electronic actuators.

See supplementary material for further details on derivations and animations MOV S1 and S2 depicting the time-evolution of the phase distribution in Figs. 4a,b, respectively.

This work is supported by start-up funds provided by the University of California.

The data that supports the findings of this study are available within the article and its supplementary material.

[1]R. W. Balluffi, S. Allen, and W. C. Carter, *Kinetics of Materials*. John Wiley & Sons, Inc., 1st ed., 2005. ISBN: 9780471246893.

[2]G. S. D. Beach, M. Tsoi, and J. L. Erskine, "Current-induced domain wall motion," *J. Magn. Magn. Mater.*, vol. 320, pp. 1272–1281, April 2008.

[3]G. Tatara, H. Kohno, and J. Shibata, "Microscopic approach to current-driven domain wall dynamics," *Phys. Rep.*, vol. 468, pp. 213–301, November 2008.

[4]D. C. Ralph and M. D. Stiles, "Spin transfer torques," *J. Magn. Magn. Mater.*, vol. 320, pp. 1190–1216, April 2008.

[5]S. S. P. Parkin, M. Hayashi, and L. Thomas, "Magnetic domain-wall racetrack memory," *Science*, vol. 320, pp. 190–194, April 2008.

[6]J. R. Raney, N. Nadkarni, C. Daraio, D. M. Kochmann, J. A. Lewis, and K. Bertoldi, "Stable propagation of mechanical signals in soft media using stored elastic energy," *Proc. Natl. Acad. Sci.*, vol. 113, pp. 9722–9727, 2016.

[7]A. Zareei, B. Deng, and K. Bertoldi, "Harnessing transition waves to realize deployable structures," *Proc. Natl. Acad. Sci.*, vol. 117, pp. 4015–4020, February 2020.

[8]B. Deng, M. Zanaty, A. E. Forte, and K. Bertoldi, "Topological solitons make metamaterials crawl," *Phys. Rev. Appl.*, vol. 17, p. 014004, January 2022.

[9]D. Melancon, A. E. Forte, L. M. Kamp, B. Gorissen, and K. Bertoldi, "Inflatable origami: multimodal deformation via multistability," *Adv. Funct. Mater.*, p. 2201891, June 2022.

[10]M. Hwang and A. Arrieta, "Topological wave energy harvesting in bistable lattices," *Smart Mater. Struct.*, vol. 31, p. 015021, January 2022.

[11]M. J. Frazier and D. M. Kochmann, "Atomimetic mechanical structures with nonlinear topological domain evolution kinetics," *Adv. Mater.*, p. 1605800, March 2017.

[12]R. Khajehtourian, M. J. Frazier, and D. M. Kochmann, "Multistable pendula as mechanical analogs of ferroelectricity," *Extreme Mech. Lett.*, vol. 50, p. 101527, January 2022.

[13]N. Nadkarni, C. Daraio, R. Abeyaratne, and D. M. Kochmann, "Universal energy transport law for dissipative and diffusive phase transitions," *Phys. Rev. B*, vol. 93, p. 104109, March 2016.

[14]N. Nadkarni, A. F. Arrieta, C. Chong, D. M. Kochmann, and C. Daraio, "Unidirectional transition waves in bistable lattices," *Phys. Rev. Lett.*, vol. 116, p. 244501, June 2016.

[15]V. Ramakrishnan and M. J. Frazier, "Transition waves in multi-stable metamaterials with space-time modulated potentials," *Appl. Phys. Lett.*, vol. 117, p. 151901, October 2020.

[16]Y. Zhou, B. G.-g. Chen, N. Upadhyaya, and V. Vitelli, "Kink-antikink asymmetry and impurity interactions in topological mechanical chains," *Phys. Rev. E*, vol. 95, p. 022202, February 2017.

[17]M. Hwang and A. F. Arrieta, "Solitary waves in bistable lattices with stiffness grading: augmenting propagation control," *Phys. Rev. E*, vol. 98, p. 042205, October 2018.

[18]L. Jin, R. Khajehtourian, J. Mueller, A. Rafsanjani, V. Tournat, K. Bertoldi, and D. M. Kochmann, "Guided transition waves in multistable mechanical metamaterials," *Proc. Natl. Acad. Sci.*, vol. 17, pp. 2319–2325, January 2020.

[19]N. Vasios, B. Deng, B. Gorissen, and K. Bertoldi, "Universally bistable shells with nonzero Gaussian curvature for two-way transition waves," *Nat. Commun.*, vol. 12, p. 695, January 2021.

[20]V. Ramakrishnan and M. J. Frazier, "Multistable metamaterial on elastic foundation enables tunable morphology for elastic wave control," *J. Appl. Phys.*, vol. 127, p. 225104, June 2020.

[21]H. Yasuda, L. M. Korpas, and J. R. Raney, "Transition waves and formation of domain walls in multistable mechanical metamaterials," *Phys. Rev. Applied*, vol. 13, p. 054067, May 2020.

[22]A. Colombi, V. Ageeva, R. J. Smith, A. Clare, R. Patel, M. Clark, D. Colquitt, P. Roux, S. Guenneau, and R. V. Craster, "Enhanced sensing and conversion of ultrasonic Rayleigh waves by elastic metasurfaces," *Sci. Rep.*, vol. 7, p. 6750, July 2017.

[23]C. Wang, A. F. Vakakis, and S. Tawfick, "Non-reciprocal frequency conversion in a two-dimensional waveguide incorporating a local nonlinear gate," *Commun. Nonlinear Sci. Numer. Simul.*, vol. 118, p. 107041, April 2023.